

Momentum-resolved charge excitations in high- T_c cuprates studied by resonant inelastic x-ray scattering

K. Ishii^{a,*} M. Hoesch^{a,b} T. Inami^a K. Kuzushita^a K. Ohwada^a M. Tsubota^a Y. Murakami^{a,c}
J. Mizuki^a Y. Endoh^{a,d} K. Tsutsui^{a,e} T. Tohyama^{f,e} S. Maekawa^{e,g} K. Yamada^e T. Masui^{h,i}
S. Tajima^{h,i} H. Kawashima^j J. Akimitsu^j

^a*Synchrotron Radiation Research Unit, Japan Atomic Energy Agency, Hyogo 679-5148, Japan*

^b*European Synchrotron Radiation Facility, 38000 Grenoble, France*

^c*Department of Physics, Graduate School of Science, Tohoku University, Sendai 980-8578, Japan*

^d*International Institute for Advanced Studies, Kizu, Kyoto 619-0025, Japan*

^e*Institute for Materials Research, Tohoku University, Sendai 980-8577, Japan*

^f*Yukawa Institute for Theoretical Physics, Kyoto University, Kyoto 606-8502, Japan*

^g*CREST, Japan Science and Technology Agency, 4-1-8 Honcho, Kawaguchi 332-0012, Japan*

^h*Department of Physics, Graduate School of Science, Osaka University, Toyonaka 560-0043, Japan*

ⁱ*Superconducting Research Laboratory, ISTEK, Tokyo 135-0062, Japan*

^j*Department of Physics and Mathematics, Aoyama-Gakuin University, Sagami-hara, Kanagawa 229-8558, Japan*

Abstract

We report a Cu K -edge resonant inelastic x-ray scattering (RIXS) study of high- T_c cuprates. Momentum-resolved charge excitations in the CuO₂ plane are examined from parent Mott insulators to carrier-doped superconductors. The Mott gap excitation in undoped insulators is found to commonly show a larger dispersion along the $[\pi, \pi]$ direction than the $[\pi, 0]$ direction. On the other hand, the resonance condition displays material dependence. Upon hole doping, the dispersion of the Mott gap excitation becomes weaker and an intraband excitation appears as a continuum intensity below the gap at the same time. In the case of electron doping, the Mott gap excitation is prominent at the zone center and a dispersive intraband excitation is observed at finite momentum transfer.

Key words: resonant inelastic x-ray scattering, charge excitation, high- T_c cuprates

1. Introduction

Strongly correlated electron systems have attracted much attention because they display a wide variety of fascinating physical properties, such as high- T_c superconductivity in cuprates. The unveiling of their electronic structure is mandatory to clarify the mechanisms underlying these physical behaviors. Essentially, one can think of the electronic structure of high- T_c cuprate superconductors as that of a doped Mott insulator in two dimensions, in which charge and spin degrees of freedom of the electron are crucial. Neutron scattering is a powerful tool to investigate the spin dynamics. On the other hand, the photon is a good probe for the charge sector. Conventional optical methods, such as optical conductivity measurement, can give infor-

mation about the momentum-conserved excitations, but momentum-resolved experiments are required for our complete understanding of the charge dynamics. Recent developments of x-ray sources from synchrotron radiation make this possible by inelastic x-ray scattering. Especially, resonant inelastic x-ray scattering (RIXS) has the advantage of element selectivity and it enables us to elucidate excitations related to the Cu orbitals by tuning the incident photon energy to the Cu K absorption edge. While angle-resolved photoemission spectroscopy (ARPES) yields one-particle excitation from the occupied state [1], RIXS provides the two-particle excitation spectra, from which one can explore both occupied and unoccupied states. In the last decade, the importance of the RIXS technique has been increasingly recognized for the investigation of the electronic structure of strongly correlated electrons systems.

In this paper, we report a comprehensive RIXS study on high- T_c cuprates from parent Mott insulators to carrier-

* Corresponding author.

Email address: kenji@spring8.or.jp (K. Ishii).

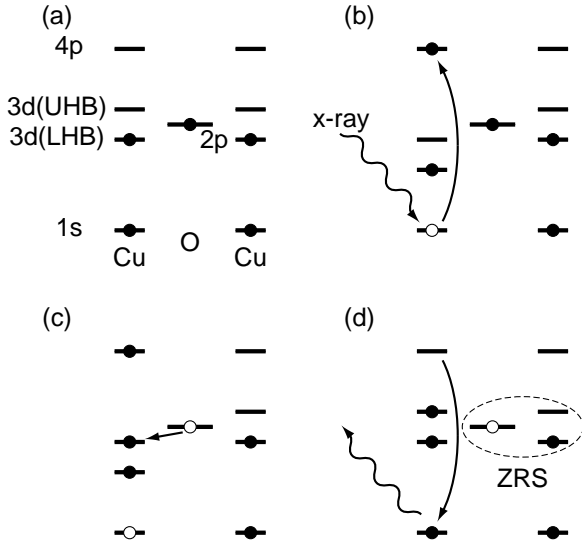


Fig. 1. Schematic energy diagram of CuO_2 plane and RIXS process at the Cu K -edge. Two Cu sites and one O $2p_\sigma$ level are shown. Filled and open circles are electron and hole, respectively.

doped superconductors. We focus on the Mott gap excitation and the intraband excitation below the gap. The latter emerges when the material is carrier doped. Evolution of the electronic structure upon carrier doping is a central issue in the physics of doped Mott insulator and we examine here how finely it can be probed using RIXS. Material dependence, including a peculiar resonance condition in Mott insulators, is discussed as well through a comparison of our results with previous work.

2. Mott gap excitation in RIXS

In this section, we briefly describe how the Mott gap excitation occurs in the RIXS process. Figures 1 show a schematic energy diagram of the CuO_2 plane and the RIXS process at the Cu K -edge. The parent materials of high- T_c superconductors are charge-transfer insulators [2]. The Cu $3d_{x^2-y^2}$ level splits into a lower Hubbard band (LHB) and an upper Hubbard band (UHB) by strong electron correlation and the O $2p_\sigma$ band is situated between them. In addition, Cu $1s$ and Cu $4p$ levels, which participate in the x-ray absorption and emission processes, are included in the diagram. Fig. 1(a) shows the ground state of a parent Mott insulator. X-ray absorption at the left Cu site brings about a dipole transition from the Cu $1s$ to the $4p$ level [Fig. 1(b)]. The $1s$ core hole predominantly scatters a valence electron. The energy of the Cu $3d_{x^2-y^2}$ of the left Cu site is lowered by an attractive Coulomb interaction with the Cu $1s$ core hole. Then an electron in the O $2p_\sigma$ transfers to the UHB to screen the core-hole potential [Fig. 1(c)]. Finally, the Cu $4p$ electron goes back to the $1s$ level again and a photon is emitted [Fig. 1(d)]. The hole in the O $2p_\sigma$ and the right Cu site form a Zhang-Rice singlet (ZRS) [3]. We call this scattering event a Mott gap excitation in the CuO_2 plane, i.e., an excitation from the ZRS band to the UHB.

3. Experimental details

The RIXS experiments were performed at BL11XU in SPring-8, where a specially designed inelastic x-ray scattering spectrometer was installed [4]. Using a Si (111) double-crystal monochromator and a Si (400) channel-cut secondary monochromator, an incident energy resolution of about 220 meV was obtained. Horizontally scattered x-rays were analyzed in energy by a spherically bent Ge (733) crystal. The total energy resolution estimated from the full width at half maximum of the elastic line was about 400 meV. All spectra were measured at room temperature.

In Continuation of our previous work on superconductors [5,6], their parent Mott insulators, Nd_2CuO_4 and $\text{YBa}_2\text{Cu}_3\text{O}_6$ were measured. We selected $\text{Ca}_{2-x}\text{Na}_x\text{CuO}_2\text{Br}_2$ as a hole doped sample. The advantage of this material in RIXS experiments is the absence of rare earth atoms that reduces the absorption of x-rays by the sample itself and a larger scattering intensity can be expected with this advantage. For the study of electron doping, we measured $\text{Nd}_{2-x}\text{Ce}_x\text{CuO}_4$.

Single crystals were prepared for all the samples. The Na concentration (x) in $\text{Ca}_{2-x}\text{Na}_x\text{CuO}_2\text{Br}_2$ was estimated as $x = 0.2$ from the superconducting transition temperature ($T_c = 14\text{K}$) [7]. $\text{YBa}_2\text{Cu}_3\text{O}_6$ and $\text{Ca}_{1.8}\text{Na}_{0.2}\text{CuO}_2\text{Br}_2$ were sealed in a beryllium cell filled with inert gas in order to avoid reaction with oxygen or water in the air.

The surface of the crystals is perpendicular to the c -axis. The crystals were mounted with the c -axis in the scattering plane. The strong two dimensionality of the electronic structure of the CuO_2 plane ensures that the momentum dependence along the c^* -axis is small. Therefore we fixed the c^* component in the absolute momentum transfer (\vec{Q}) at a value where the scattering angle (2θ) is close to 90° . This enables us to reduce the elastic scattering by the polarization factor of the Thomson scattering [6]. We measured the momentum dependence of the CuO_2 plane in the transverse geometry. A schematic view of the RIXS experimental configuration is shown in the inset of Fig. 2(d). The polarization of the incident x-rays ($\vec{\epsilon}_i$) contains nearly equal out-of-plane ($\vec{\epsilon}_i \parallel \vec{c}$) and in-plane ($\vec{\epsilon}_i \perp \vec{c}$) components.

4. Results and Discussion

4.1. Incident energy dependence and resonance condition of the Mott insulators

Figures 2(a) and (b) show the incident energy dependence of the RIXS spectra of Nd_2CuO_4 and $\text{YBa}_2\text{Cu}_3\text{O}_6$, respectively. The reduced momentum transfer in the ab plane (\vec{q}) is $(\pi, 0)$. The spectral weight around 2 eV arises from the excitation across the Mott gap and its intensity is resonantly enhanced at some incident energies.

Because the intermediate state of RIXS corresponds to the final state of x-ray absorption, it is interesting to compare absorption spectra with the incident photon

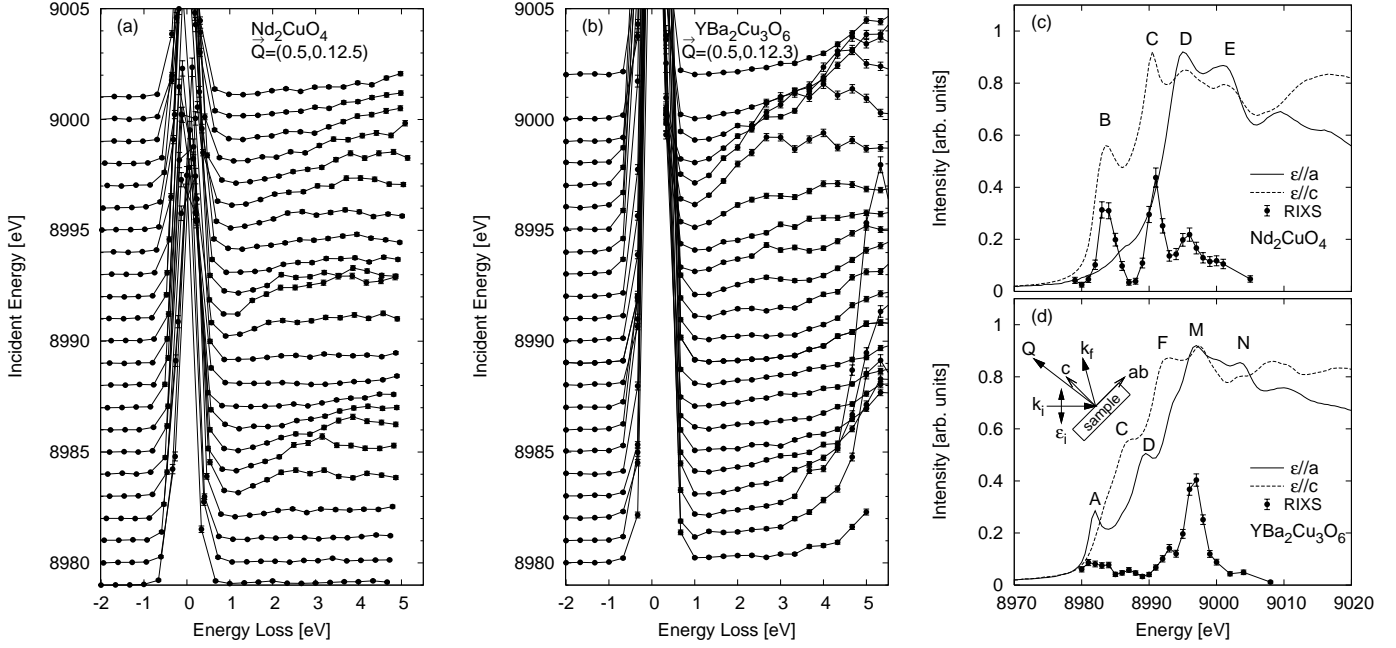


Fig. 2. Incident photon energy dependence of RIXS spectra of (a) Nd_2CuO_4 and (b) $\text{YBa}_2\text{Cu}_3\text{O}_6$. The absolute momentum transfer is $\vec{Q} = (0.5, 0, 12.5)$ and $(0.5, 0, 12.3)$ for Nd_2CuO_4 and $\text{YBa}_2\text{Cu}_3\text{O}_6$, respectively. The incident energy for each scan can be read from the vertical axis. X-ray absorption spectra of (c) Nd_2CuO_4 and (d) $\text{YBa}_2\text{Cu}_3\text{O}_6$. RIXS intensities integrated between 1 and 3 eV are also shown as a function of the incident photon energy.

energy dependence of RIXS. Solid and dashed lines in Figs. 2(c) and (d) are the absorption spectra of Nd_2CuO_4 and $\text{YBa}_2\text{Cu}_3\text{O}_6$ obtained by the total fluorescence yield. Prominent peaks in the absorption spectra are labeled by the same letters A-N as in the reports [8,9]. In Nd_2CuO_4 , the peaks B and C in the $\epsilon \parallel c$ spectrum are assigned to the $1s-4p_\pi$ transitions. The peaks D and E in the $\epsilon \parallel a$ spectrum are the $1s-4p_\sigma$ transitions. In each pair, the peaks at lower energy (B and D) and those at higher energy (C and E) correspond to well-screened and poorly-screened core-hole final states, respectively [8]. On the other hand, the assignment of the features in the $\text{YBa}_2\text{Cu}_3\text{O}_6$ spectra is rather complicated [9] because there are two distinct Cu sites. One type of Cu atoms is in the monovalent Cu(1) site, which forms the one-dimensional chains in $\text{YBa}_2\text{Cu}_3\text{O}_{7-x}$. The other is the divalent Cu(2) site in the CuO_2 plane. The peaks of A and D in the $\epsilon \parallel a$ spectrum are absent in $\text{YBa}_2\text{Cu}_3\text{O}_{6.95}$ and they are attributed to the transitions at the Cu(1) sites. The peak A is a proof of the existence of a monovalent Cu atom [10,11]. The peaks M and N are the $1s-4p_\sigma$ transitions of the Cu(2) site. A pair of peaks of the $1s-4p_\pi$ transitions of the Cu(2) site should appear in the $\epsilon \parallel c$ spectrum. It can be assigned to the peaks C and F but the $1s-4p_\sigma$ transition of the Cu(1) site may overlap.

In $\text{YBa}_2\text{Cu}_3\text{O}_6$, a large RIXS intensity is observed around 5 eV when the incident photon energy is close to the peak A in the absorption spectra, indicating that this excitation is related to the Cu(1) site. In order to show the resonant feature of the Mott gap excitation more precisely, the RIXS intensity in Fig. 2 (a) and (b) is integrated between 1 and 3 eV and plotted as a function of the incident

photon energy in Figs. 2(c) and (d). Clear difference is observed in the incident energy profile of the Mott gap excitation between Nd_2CuO_4 and $\text{YBa}_2\text{Cu}_3\text{O}_6$, that is, there are three well-pronounced resonances for the former and only one peak with a bump on the lower-energy side for the latter. Each resonant energy of the RIXS intensity is found to correspond to a peak in the absorption spectra. We note that both out-of-plane ($\vec{\epsilon}_i \parallel \vec{c}$) and in-plane ($\vec{\epsilon}_i \perp \vec{c}$) components coexist in the incident photon polarization in our experimental condition. In contrast to the two cases, La_2CuO_4 shows two distinct resonances with respect to the polarization condition; one is at $E_i = 8990$ eV in the out-of-plane condition and the other is at $E_i = 8994$ eV in the in-plane condition [12].

As shown in Fig. 1, the screening process by the charge transfer from the ligand oxygen to the UHB in the intermediate state is important for the Mott gap excitation. This means that the Mott gap excitation is enhanced when the incident energy is tuned to the well-screened state in the x-ray absorption spectra [13,14]. This rule is applicable to La_2CuO_4 [12] as well as to the in-plane condition of Nd_2CuO_4 [peak D in Fig. 2(c)] and $\text{YBa}_2\text{Cu}_3\text{O}_6$ [peak M in Fig. 2(d)]. In contrast, two resonances appear in the out-of-plane condition of Nd_2CuO_4 [peak B and C in Fig. 2(c)]. In the configuration-interaction picture, the well-screened and poorly-screened states are expressed by linear combinations of $|\underline{1s}, 3d^9, 4p_\pi\rangle$ and $|\underline{1s}, 3d^{10}, \underline{L}, 4p_\pi\rangle$, where $\underline{1s}$ and \underline{L} denote a hole in $1s$ level and ligand oxygen, respectively. Generally, $|\underline{1s}, 3d^{10}, \underline{L}, 4p_\pi\rangle$ is dominant in the well-screened state. The two resonances in the out-of-plane condition of Nd_2CuO_4 indicate that $|\underline{1s}, 3d^{10}, \underline{L}, 4p_\pi\rangle$ has relatively

large weight at the absorption labeled C in Fig. 2(c), though it has been assigned to the poorly-screened state. We have no explanation for the weakness or disappearance of the resonance in the out-of-plane condition of $\text{YBa}_2\text{Cu}_3\text{O}_6$ so far. It may be related to a structural difference, namely, the Cu atom in the CuO_2 plane is fivefold coordinated by four planar and one apical oxygens in $\text{YBa}_2\text{Cu}_3\text{O}_6$, which breaks the mirror symmetry perpendicular to the c -axis, while the symmetry is present in La_2CuO_4 and Nd_2CuO_4 . Further systematic studies are necessary to understand the difference in the out-of-plane condition.

4.2. Momentum dependence of the Mott insulators

Figures 3 (a) and (b) show the momentum dependence of Nd_2CuO_4 and YBa_2CuO_6 , respectively. The incident photon is fixed at the resonance energy derived from Figs. 2. The RIXS intensity is almost zero at ~ 1 eV and a clear Mott gap can be seen at all momenta. Taking advantage of the experimental condition of $2\theta \simeq 90^\circ$, the gap is much clearer in our spectra than that in the previous RIXS works on parent materials, $\text{Ca}_2\text{CuO}_2\text{Cl}_2$ [17] and La_2CuO_4 [16] where the scattering intensity below the gap does not reach close to zero due to the tail of the elastic scattering.

Here, we discuss the momentum dependence of the overall spectral weight rather than that of the peak positions. A recent detailed study of $\text{HgBa}_2\text{CuO}_{4+\delta}$ and La_2CuO_4 demonstrated that a multiplet of peaks with a weak dispersion can be elucidated by utilizing the subtle dependence of the cross section on the incident photon energy [18,12]. Though the peak position of each peak shows a weak dispersion, the overall spectral weight containing the intensity of the multiplet shifts as a function of momentum transfer. Moreover, such a multiplet is not clearly observed in our data, which may be due to different experimental conditions with Ref. [18,12], such as polarization and absolute momentum transfer. Focusing on the spectral weight, we notice from Figs. 3 (a) and (b) that the changes in the excitation spectra are small along the $[\pi, 0]$ direction while the spectral weight clearly shifts to higher energy as the momentum transfer increases along the $[\pi, \pi]$ direction. The center of gravity of the RIXS spectra between 1 and 4 eV is plotted as a function of momentum transfer in Fig. 3(c), which corresponds to the dispersion relation of the spectral weight of the Mott gap excitation. The momentum dependence of the Mott gap excitation shows a large anisotropy; the dispersion along the $[\pi, \pi]$ direction is larger than that along the $[\pi, 0]$ direction.

The larger dispersion along the $[\pi, \pi]$ direction was predicted by a theoretical calculation based on a single band Hubbard model with long range hoppings (t - t' - t'' - U model) [19]. Besides, it has been experimentally observed in $\text{Ca}_2\text{CuO}_2\text{Cl}_2$ [17]. In La_2CuO_4 [16], the authors claimed that the spectral weight of the lowest excitation (labeled A in the reference) becomes small at $\vec{q} = (\pi, \pi)$ and this results in a shift of the spectral weight to higher energy.

In Fig. 3(d), we compare the RIXS spectra of La_2CuO_4 in Ref. [16] with our data. The momentum dependence of La_2CuO_4 is qualitatively similar to that of Nd_2CuO_4 and $\text{YBa}_2\text{Cu}_3\text{O}_6$. Therefore, we conclude that the larger dispersion along the $[\pi, \pi]$ direction than that along the $[\pi, 0]$ direction is a common character of the Mott gap excitation in the insulating CuO_2 plane.

Quantitatively, the RIXS spectra depend on the material. Comparing the spectra at the zone center in Fig. 3(d), the gap energy is found to systematically change with the number of oxygens coordinated around Cu, that is, it is largest in the octahedral structure of La_2CuO_4 and smallest in the square structure of Nd_2CuO_4 . $\text{YBa}_2\text{Cu}_3\text{O}_6$, with its pyramidal coordination geometry, lies between the two. This systematic change of the gap has been already reported from an optical conductivity experiment [20], which is consistent with our RIXS results.

The magnitude of the dispersion also displays material dependence. Experimentally, the dispersion along the $[\pi, 0]$ direction is apparent in La_2CuO_4 [16,12,15], while that of Nd_2CuO_4 and $\text{YBa}_2\text{Cu}_3\text{O}_6$ is fairly small. The dispersion of La_2CuO_4 in Ref. [15], where momentum-dependent RIXS spectra along the $[\pi, 0]$ direction are presented, is superimposed in Fig. 3(c). We can also ascertain from the spectral weight that the dispersion along $[\pi, 0]$ direction is larger in La_2CuO_4 . On the other hand, it is demonstrated theoretically that the long-range hoppings t' and t'' play an important role for the dispersion of RIXS spectra [19,21]; the dispersion along the $[\pi, 0]$ direction becomes larger without t' and t'' . Accordingly, our experimental results suggest that long range hopping parameters of Nd_2CuO_4 and $\text{YBa}_2\text{Cu}_3\text{O}_6$ are larger than those of La_2CuO_4 . Comparing relatively between Nd_2CuO_4 and La_2CuO_4 , it is consistent with the parameters which are obtained from the shape of the Fermi surface in ARPES experiments [22]. Furthermore the experimental result that $\text{YBa}_2\text{Cu}_3\text{O}_6$ has larger long range hopping than La_2CuO_4 agrees with a theory which proposed that materials with higher T_c at optimal doping have larger hopping term [23].

4.3. Carrier-doping effect

In this section, we discuss RIXS spectra of carrier-doped superconductors and compare them with those of Mott insulators. Fig. 4(a) shows the momentum dependence of RIXS spectra obtained for hole-doped $\text{Ca}_{1.8}\text{Na}_{0.2}\text{CuO}_2\text{Br}_2$. The incident photon energy is 8984 eV which corresponds to the well-screened state of the out-of-plane condition in the absorption spectrum. A large spectral weight remains located above 2 eV, which indicates that the Mott gap persists even in the hole-doped superconductor. At the same time, the gap is filled by a continuum intensity below 2 eV. While the former excitation is the interband excitation across the Mott gap, the latter is related to the dynamics of doped holes in the Zhang-Rice singlet band and we call it intraband excitation.

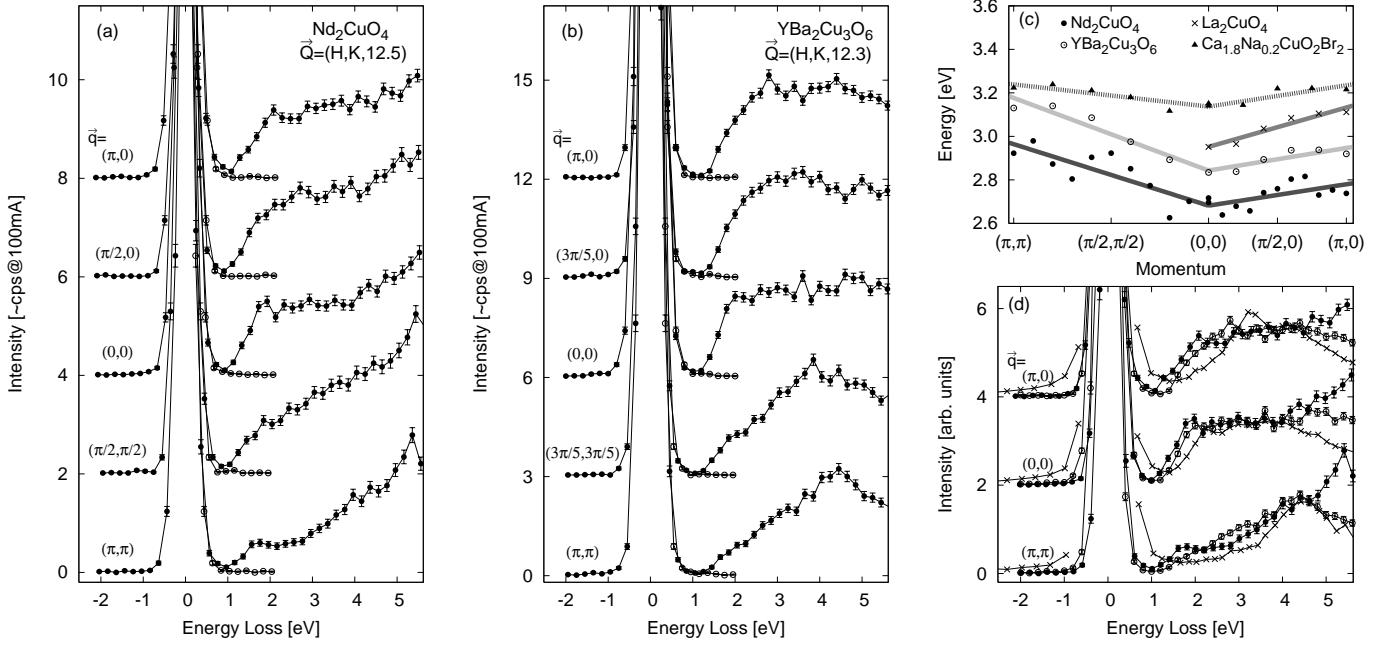


Fig. 3. Momentum dependence of RIXS spectra of (a) Nd_2CuO_4 , (b) $\text{YBa}_2\text{Cu}_3\text{O}_6$. The incident photon energy is 8991 eV for Nd_2CuO_4 and 8996 eV for $\text{YBa}_2\text{Cu}_3\text{O}_6$. Filled circles are the raw data. The data in the anti-Stokes region are folded at the origin and plotted as open circles, from which we can estimate the elastic tail and the background. (c) Momentum dependence of the Mott gap excitation. The center of gravity of the RIXS spectra between 1 and 4 eV is plotted for Nd_2CuO_4 , $\text{YBa}_2\text{Cu}_3\text{O}_6$, and La_2CuO_4 . The data of La_2CuO_4 are taken from the Ref. [15]. For $\text{Ca}_{1.8}\text{Na}_{0.2}\text{CuO}_2\text{Br}_2$, the center of gravity between 2 and 4 eV is used to exclude contribution from the intraband excitation. The thick lines are drawn assuming a linear dispersion. (d) Comparison of three Mott insulators. The symbols are the same as in (c). The data of La_2CuO_4 are taken from the Ref. [16].

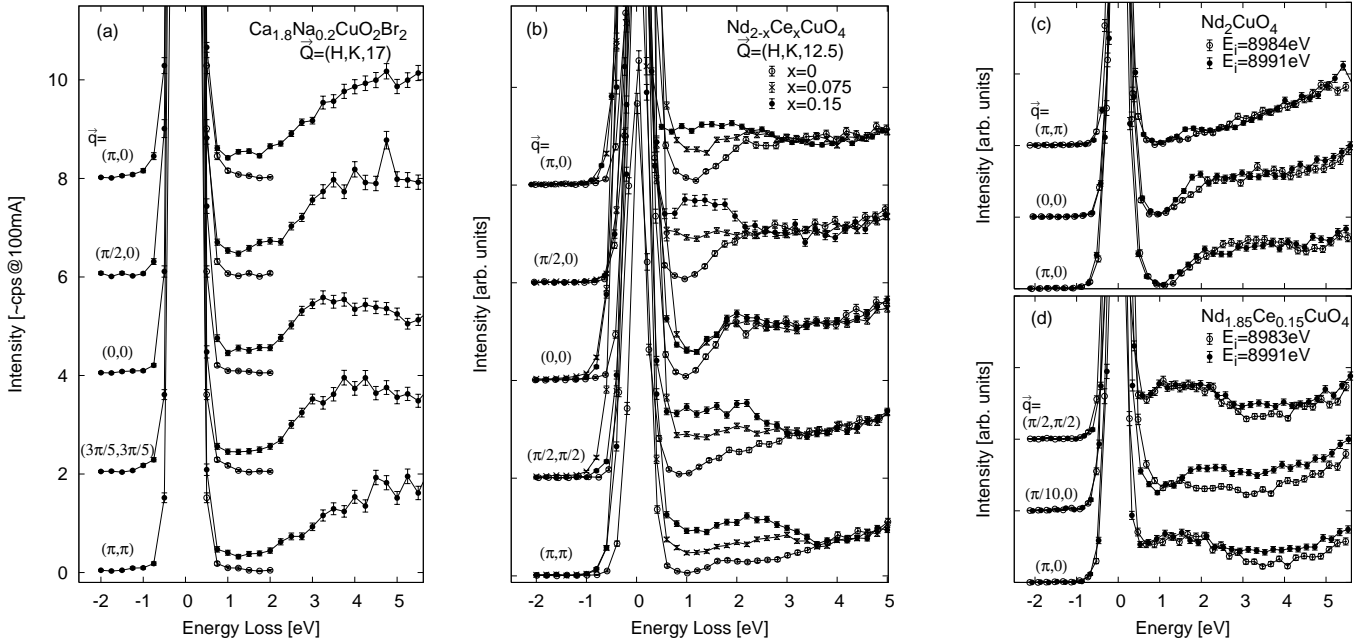


Fig. 4. (a) RIXS spectra of hole-doped $\text{Ca}_{1.8}\text{Na}_{0.2}\text{CuO}_2\text{Br}_2$. The incident photon energy is 8984 eV. Filled circles are the raw data. The data in the anti-Stokes region are folded at the origin and plotted as open circles. (b) RIXS spectra of $\text{Nd}_{2-x}\text{Ce}_x\text{CuO}_4$, which show electron-doping dependence. The incident photon energy is 8991 eV. (c) and (d) Comparison of RIXS spectra of Nd_2CuO_4 and $\text{Nd}_{1.85}\text{Ce}_{0.15}\text{CuO}_4$ measured at two incident photon energies.

When the interband excitation of $\text{Ca}_{1.8}\text{Na}_{0.2}\text{CuO}_2\text{Br}_2$ is compared with that of Mott insulators, the spectral weight around 2 eV decreases by hole doping except for the spectrum at $\vec{q} = (\pi, \pi)$ where the intensity around 2 eV is weak even in Mott insulators. As a result, the total spectral weight of the interband excitation shifts to higher energy and the dispersion becomes weaker. In Fig. 3(c), the center of gravity of the spectral weight between 2-4 eV is shown as a function of momentum. It is apparent that the dispersion is weaker in the hole-doped $\text{Ca}_{1.8}\text{Na}_{0.2}\text{CuO}_2\text{Br}_2$ than in the Mott insulators. Such a change is also observed in $\text{La}_{2-x}\text{Sr}_x\text{CuO}_4$ [24]; a well-defined peak feature at 2-3 eV for $x = 0$ (labeled A in Ref. [16]) decreases in intensity or disappears at $x = 0.17$ and the overall spectral weight (labeled AB in Ref. [24]) shows weaker dispersion. Furthermore, the excitation from the CuO_2 plane in optimally-doped $\text{YBa}_2\text{Cu}_3\text{O}_{7-\delta}$ also shows very weak dispersion [5,25].

These characteristic changes of the Mott gap excitation by hole doping are consistent with a theoretical prediction [26,21]. The shift of the spectral weight to higher energy is attributed to a shift of the Fermi energy upon hole doping. On the other hand, it is suggested in the theory that the weaker dispersion in the hole-doped case compared with that in the undoped case is related to the reduction of antiferromagnetic correlation. With realistic parameters used in the theory, the antiferromagnetic correlation is strongly suppressed by hole doping and the dispersion of the Mott gap excitation becomes weaker. In contrast, the short-range antiferromagnetic correlation is kept in the electron-doped case, and the magnitude of the dispersion of the Mott gap excitation is almost the same as that of the undoped case. This result indicates that the underlying magnetism governs the charge dynamics in the high-energy region up to a few eV. It is noted that the two-leg ladder shows a different behavior upon hole doping. A recent RIXS study of $(\text{La}, \text{Sr}, \text{Ca})_{14}\text{Cu}_{24}\text{O}_{41}$ demonstrated that the momentum dependence of the Mott gap excitation in the two-leg ladder is insensitive to the hole doping as well as the spin gap state [27].

Next, we discuss the results of electron doping. In Fig. 4(b), RIXS spectra for the $x = 0, 0.075$, and 0.15 in samples of $\text{Nd}_{2-x}\text{Ce}_x\text{CuO}_4$ are compared. The incident photon energy is fixed at 8991 eV for all samples. The spectra are normalized to the intensity at 4-5 eV. The doping dependence is apparently different between the zone center and finite \vec{q} . At the zone center, the Mott gap excitation at 2 eV is unchanged upon electron doping, which means that the charge gap due to the electron correlation persists even in the metallic phase.

Two theoretical calculations of the electron doped CuO_2 plane have been reported. One is based on a single band Hubbard model using a numerically exact diagonalization technique on a small cluster [26]. The other adopts a d - p model and the Hartree-Fock approximation is applied [28]. In the former theory, the Mott gap excitation persists upon electron doping, and especially, it is enhanced in the spec-

trum at the zone center. On the other hand, the latter suggests a collapse of the gap. Our experimental observation of the 2 eV feature remaining in the electron-doped metallic state supports the validity of the former theory.

At finite momentum transfer, large spectral weight appears below the gap. Its intensity is roughly proportional to the number of doped electrons (x). Hence it is related to the intraband dynamics of the doped electrons in the UHB. Because details of the intraband excitation have already been published [6,29], we do not discuss them here.

Finally, we show the difference of resonance conditions between the undoped and electron-doped cases. In Fig. 4(c), RIXS spectra measured at two incident photon energies are compared for Nd_2CuO_4 . The lower 8984 eV is close to the well-screened state of the out-of-plane condition [peak B in Fig. 2(c)], while the higher 8991 eV corresponds to the poorly-screened state [peak C in Fig. 2(c)]. The scale factors are common for the spectra at the three momenta. The spectra strongly resemble between the two incident photon energies. On the other hand, the spectra of $\text{Nd}_{1.85}\text{Ce}_{0.15}\text{CuO}_4$ in Fig. 4(d) show a difference near the zone center, $\vec{q} = (\pi/10, 0)$; the 2 eV feature is suppressed at 8983 eV. This is an additional proof that the excitation at 2 eV at the zone center is qualitatively different from the intraband excitation observed at the finite momentum transfer. In the electron-doped case, only the intraband excitation is expected to be enhanced at the incident photon energy where the core hole is created at the doped site [6,21]. This energy should exist below the well-screened state and 8983 eV in $\text{Nd}_{1.85}\text{Ce}_{0.15}\text{CuO}_4$ may be close to it.

5. Summary

We have performed a Cu K -edge RIXS study of high- T_c cuprates from parent Mott insulators to carrier-doped superconductors. While the resonance condition depends on materials, an anisotropic dispersion, that is, larger dispersion along the $[\pi, \pi]$ direction than the $[\pi, 0]$ direction, is commonly observed in undoped Mott insulators. Upon hole doping, the dispersion of the Mott gap excitation becomes weaker, while the Mott gap excitation is prominent at the zone center in the electron doped case. At the same time, an intraband excitation emerges below the gap in both hole- and electron-dopings. These characteristics are consistent with a theoretical calculation based on the Hubbard model.

Acknowledgments The authors thank Dr. I. Jarrige for proofreading of the manuscript. This work was performed under the inter-university cooperative research program of the Institute of Materials Research, Tohoku University and financially supported by the Grant-in-Aid for Scientific Research on Priority Areas "Invention of anomalous quantum materials" from the Ministry of Education, Culture, Sports, Science, and Technology of Japan. K. I. was also supported

by Grant-in-Aid for Young Scientists from JSPS. The crystal growth of $\text{YBa}_2\text{Cu}_3\text{O}_6$ was supported by the New Energy and Industrial Technology Development Organization (NEDO) as the Collaborative Research and Development of Fundamental Technologies for Superconductivity Applications.

References

- [1] A. Damascelli, et al., Rev. Mod. Phys. 75 (2003) 473.
- [2] J. Zaanen, et al., Phys. Rev. Lett. 55 (1985) 418.
- [3] F. C. Zhang, et al., Phys. Rev. B 37 (1988) 3759.
- [4] T. Inami, et al., Nucl. Instrum. Methods Phys. Res. A 467-468 (2001) 1081.
- [5] K. Ishii, et al., Phys. Rev. Lett. 94 (2005) 187002.
- [6] K. Ishii, et al., Phys. Rev. Lett. 94 (2005) 207003.
- [7] S. Kuroiwa, et al., Physica B 374-375 (2006) 75.
- [8] N. Kosugi, et al., Phys. Rev. B 41 (1990) 131.
- [9] H. Tolentino, et al., Physica C 192 (1992) 115.
- [10] S. M. Heald, et al., Phys. Rev. B 38 (1988) 761.
- [11] J. M. Tranquada, et al., Phys. Rev. B 38 (1988) 8893.
- [12] L. Lu, et al., Phys. Rev. B 74 (2006) 224509.
- [13] T. Idé, et al., J. Phys. Soc. Jpn. 68 (1999) 3100.
- [14] T. Idé, et al., J. Phys. Soc. Jpn. 69 (2000) 3107.
- [15] E. Collart, et al., Phys. Rev. Lett. 96 (2006) 157004.
- [16] Y. J. Kim, et al., Phys. Rev. Lett. 89 (2002) 177003.
- [17] M. Z. Hasan, et al., Science 288 (2000) 1811.
- [18] L. Lu, et al., Phys. Rev. Lett. 95 (2005) 217003.
- [19] K. Tsutsui, et al., Phys. Rev. Lett. 83 (1999) 3705.
- [20] Y. Tokura, et al., Phys. Rev. B 41 (1990) 11657.
- [21] T. Tohyama, et al., J. of Phys. Chem. Solids 66 (2005) 2139.
- [22] T. Tohyama, et al., Supercond. Sci. Technol. 13 (2000) R17.
- [23] E. Pavarini, et al., Phys. Rev. Lett. 87 (2001) 047003.
- [24] Y.-J. Kim, et al., Phys. Rev. B 70 (2004) 094524.
- [25] K. Ishii, et al., AIP Conf. Proc. 850 (2006) 445.
- [26] K. Tsutsui, et al., Phys. Rev. Lett. 91 (2003) 117001.
- [27] K. Ishii, et al., Phys. Rev. B 76 (2007) 045124.
- [28] R. S. Markiewicz, et al., Phys. Rev. Lett. 96 (2006) 107005.
- [29] K. Ishii, et al., AIP Conf. Proc. 850 (2006) 403.